Regulatory Mechanisms in Biosystems

ISSN 2519-8521 (Print)
ISSN 2520-2588 (Online)
Regul. Mech. Biosyst.

Characterization of *Sorbus aria*-mediated silver nanoparticles and evaluation of antibacterial activity against *Staphylococcus epidermidis* clinical strains

N. O. Khromykh*, O. O. Didur*, T. V. Sklyar*, L. Procházková**,
L. Nedbalová**, J. Nebesarova**, O. K. Balalaiev***, N. V. Kuragina*

**Oles Honchar Dnipro National University, Dnipro, Ukraine*
*** Charles University, Prague, Czech Republic*
****M. S. Polyakov Institute of Geotechnical Mechanics NAS of Ukraine, Dnipro, Ukraine*

Article info

Received 20.02.2025
Received in revised form 19.03.2025
Accepted 10.04.2025

Oles Honchar Dnipro National University, Nauky av., 72, Dnipro, 49045, Ukraine. Tel.:+38-050-487-87-17. E-mail: khromykh2012@gmail.com

Charles University, Faculty of Science, Viničná st., 7, Prague, Czech Republic.

M. S. Polyakov Institute of Geotechnical Mechanics NAS of Ukraine, Simferopol's'ka st., 2a, Dnipro, 49005, Ukraine.

Khromykh, N. O., Didur, O. O., Sklyar, T. V., Procházková, L., Nedbalová, L., Nebesarova, J., Balalaiev, O. K., & Kuragina, N. V. (2025). Characterization of Sorbus aria mediated silver nanoparticles and evaluation of antibacterial activity against Staphylococcus epidermidis clinical strains. Regulatory Mechanisms in Biosystems, 16(2), e25056. doi:10.15421/0225056

Biosynthesis of silver nanoparticles (AgNPs) using plant extracts serves as an attractive environmentally friendly and cost-effective alternative to the traditional methods of producing nanomaterials with antimicrobial properties. This article characterizes AgNPs derived from an aqueous leaf extract of *Sorbus aria* plants (Sa-AgNPs), and presents the results of their testing against antibiotic-resistant clinical bacterial strains. The formation of silver nanoparticles was observed visually according to the change in the color of solution and was confirmed by the induced plasmon resonance peak, recorded by UV-Vis spectroscopy at 450 nm. According to the TEM imaging, the biosynthesized Sa-AgNPs were spherical, with an average size of 47.5 nm, and exhibited a moderate polydispersity, with the PDI calculated as 0.138. The SEM images confirmed the spherical shape of the Sa-AgNPs and the absence of their agglomeration. The phytochemicals from the plant matrix that served as reducing, stabilizing, and capping agents for Sa-AgNPs biosynthesis were identified using Fourier transform infrared spectroscopy as phenolics, alcohols, terpenes, and proteins, with hydroxyl, carbonyl, carboxyl, and amines being the responsible functional groups. The antibacterial activity of the biosynthesized silver nanoparticles was examined using the disc diffusion method against two clinically isolated *Staphylococcus epidermidis* strains that differed in sensitivity to some antibiotics from several classes. The growth inhibition of both *S. epidermidis* strains by Sa-AgNPs was dose-dependent at a concentration range of 15.625–1,000 µg/mL. The *S. epidermidis* strain that displayed a stronger resistance to several fluoroquinolones, cephalosporines and aminoglycosides, showed higher susceptibility to the antibacterial action of Sa-AgNPs than the less drug-resistant strain. The hemolytic assay revealed a good biological compatibility of the biosynthesized Sa-AgNPs at concentrations of up to 25 µg/mL. The study results confirmed the potential ability of phytosynthesized silver nanoparticles to achieve considerable success in the fight against antibiotic resistance of *S. epidermidis*. Further research is needed to test a large number of resistant clinical strains to clarify the suitability of Sa-AgNPs for development of new antibacterial drugs.

Keywords: phytosynthesis; AgNPs; antibiotic resistance; bacterial growth inhibition; SEM; TEM; FTIR; hemolytic test.

Introduction

Nowadays, nanomaterials are used in various fields of medicine, and are considered as one of the possible means of overcoming antibiotic resistance of pathogenic microorganisms (Salem, 2023; Osman et al., 2024; Yadav & Yadav, 2025). Silver nanoparticles (AgNPs) are among the most frequently synthesized and studied metallic nanoparticles, as they differ from the natural substances by a larger ratio between volume and surface, which increases their biological activity, in particular, the ability to inhibit the growth of microorganisms (Mihailović et al., 2023; Akhter et al., 2024). Since the antibacterial effects of silver nanoparticles are realized not only at the cellular level, but also through their effects on many bacterial structures and metabolic processes at the same time, AgNPs pose a low risk of developing bacterial resistance (More et al., 2023; Summer et al., 2024). The antimicrobial effectiveness of silver nanoparticles has been confirmed in the numerous tests against Gram-positive and Gram-negative bacteria and fungal strains (Al-Rajhi et al., 2022; Didur et al., 2024; Lykholat et al., 2025). However, the search for alternative antimicrobial agents remains relevant, since numerous pathogenic strains with reduced or completely lost sensitivity to conventional antibiotics have been reported in recent decades (Sánchez-López et al., 2020; Khan et al., 2024).

Resistance of microorganisms to one or more antibiotics has arisen in different countries due to the incorrect and excessive use of drugs over a long period (Cook & Wright, 2022). Furthermore, the effectiveness of conventional antibiotics has been lost due to the operation of sophisticated evasion mechanisms in pathogenic microbes, which makes infections increasingly difficult to treat. Mechanisms that confer the bacterial antibiotic resistance include drug inactivation by bacterial enzymes, followed by the drug degradation; drug target modification; cell wall modification, leading to inhibition of drug uptake; the active efflux of drugs via efflux pumps; and drug resistance gene in the bacterial plasmid (Wiart et al., 2023; Summer et al., 2024). The spread of antibiotic-resistant microorganisms increases the danger of bacterial infections. According to a clinical impact research (Ghai, 2024), resistant infections are associated with increased morbidity, mortality, and healthcare costs. Unfortunately, since a proven countermeasure to antibiotic resistance has not been found yet, Vazquez-Muñoz et al. (2019) stated that the evolution of multiresistant bacteria occurs faster than the development of new effective antibiotics.

One of the commonest microbes in the clinical space is *Staphylococcus epidermidis*, which can behave as a pathogen, colonizing medical devices, infecting surgical wounds, and causing bacteremia (Asante et al., 2021). Although *S. epidermidis* has traditionally been considered an opportunistic bacterium found in the normal skin microbiota, it often becomes resistant to antibiotics. In particular, Oliver et al. (2022) found methicillin-resistant strains of *S. epidermidis* (MRSE) to be a frequent cause of keratitis, detected in over 37% of the cases. Moreover, *S. epidermidis* can be resistant to β-lactams, and often acquires resistance to other ophthalmic antibiotics such as quinolones or tetracyclines. Such a threatening trend represents a serious problem related not only to ophthalmic diseases, but also to systemic infections. Given the current lack of new antibiotics in development, recently noted by Paul et al. (2023), it is necessary to find alternative

strategies to combat microbial drug resistance. One of the promising approaches for overcoming bacterial resistance can be the use of the antimicrobial potential of silver nanoparticles (Ewunkem et al., 2023).

The synthesis of silver nanoparticles has traditionally been carried out by chemical and physical means; however, the use of innovative biological (green) synthesis, which is characterized as safe, simple, cost-effective, and environmentally friendly, opens up new opportunities for obtaining AgNPs (Akhter et al., 2024; Osman et al., 2024). The main advantage of green synthesis of nanoparticles is that biological extracts, including plant-derived, contain various biomolecules, such as proteins, amino acids, polysaccharides, phenolic compounds, flavonoids, tannins, saponins, terpenoids, and alkaloids, which ensure the processes of reducing, stabilization, and capping of nanoparticles (Hemmati et al., 2019; Reda et al., 2019; Karan et al., 2024). Biosynthesized silver nanoparticles are highly stable (Raj et al., 2018), biocompatible (Hossain et al., 2019), and low-toxic due to the formation of a biological corona on the surface of the developed nanoparticles (More et al., 2023). In addition, comparative studies have shown that silver nanoparticles synthesized biologically from plant and fungal extracts displayed better antibacterial activity against Gram-negative and Gram-positive pathogenic bacteria than nanoparticles synthesized chemically (Aguirre et al., 2020).

In our study, the phytochemicals of the *Sorbus aria* leaves were used as reducing, stabilizing, and capping agents for the synthesis of nanoparticles. Plants of the *Sorbus* L. genus are widely known in ethnomedicine as a source of biologically active compounds suitable for the treatment of bacterial, viral, inflammatory diseases, including tumors (Sarv et al., 2020; Orsavová et al., 2023). Studies of phytochemical composition of the *Sorbus* plants revealed a high content of secondary metabolites, such as caffeylquinic acids, in particular, chlorogenic, neochlorogenic, caffeic (Bobinaitė et al., 2020), and ferulic (Tas et al., 2023); flavonoids (Tahirovic et al., 2019), including quercetin, rutin, hyperoside, catechin, procyanidins (Rutkowska et al., 2019; Arvinte et al., 2023); and terpenoids (Sołtys et al., 2020; Lykholat et al., 2024). The presence of a rich complex of metabolites indicates the potential suitability for AgNPs biosynthesis and determines the expediency of testing *Sorbus* plants. To date, only the *Sorbus aucuparia* fruits have been used for the biosynthesis of silver nanoparticles, which exhibited a high activity against Gram-negative bacteria (Singh & Mijakovic, 2022). The objectives of our study were carrying out a biogenic synthesis of silver nanoparticles using an aqueous leaf extract of *S. aria* and testing the ability of the biosynthesized nanoparticles to inhibit clinically isolated drug-resistant *S. epidermidis* strains.

Materials and methods

Materials. The silver nitrate (99.9% purity) and Triton X-100 were purchased from Sigma-Aldrich. We used sterile paper discs loaded with fluoroquinolone, cephalosporine, and aminoglycoside antibiotics manufactured by Disk-Aspect (Ukraine); pure sterile paper discs; and Meat Peptone Agar RM1049 from HiMedia Laboratories Pvt. Limited (India).

Collection of plant material and preparation of plant extract. The leaves of *Sorbus aria* plants were collected in May 2024 in the Botanical Garden of Oles Honchar Dnipro National University (48°26'7" N, 35°2'34" E, Dnipro, Ukraine). The plant material was washed with distilled water, dried in the shade, crushed using a mortar and pestle, and sieved through a 2 mm mesh. To prepare the aqueous leaf extract of *S. aria*, a 1.5 g sample of dry plant mass in a 100 mL conical flask was supplemented with 30 mL distilled water, heated in a water bath to 60 ºC and kept for 60 min. After cooling and settling for two hours, the extract was centrifuged at 12,000 rpm for 15 min, and the supernatant was used for the green synthesis.

Phytosynthesis of Sa-AgNPs. The production of silver nanoparticles based on *S. aria* leaf extract (Sa-AgNPs) was carried out according to an optimized procedure, mixing the plant extract with 25 mmol/L aqueous solution of $AgNO_3$ in a ratio of 5:1 (v/v). The formation of Sa-AgNPs was visually observed as the solution color changed from yellow to brown after incubation at 37 °C for 3 hours. To remove plant residues, the colloidal solution of silver nanoparticles was mixed with distilled water (1:5, v/v) and centrifuged at 12,000 rpm for 15 min, repeating the procedure two times. The supernatants were removed, and the precipitates containing Sa-AgNPs were stored fridge at 4 ºC and used for the further study.

Ultraviolet-visible spectroscopy. The presence of silver nanoparticles in the colloidal solution of phytosynthesized Sa-AgNPs was confirmed by a UV-Vis spectroscopic analysis. To obtain the UV-Vis spectra of the Sa-AgNPs, the colloidal solution was diluted (1:20) in distilled water, and the absorbance was measured using a NanoDrop Micro-UV/Vis spectrophotometer (Thermo Fisher Scientific Inc., USA) in a wavelength range of 200–800 nm.

Transmission electron microscopy (TEM). The shape and size of the phytosynthesized Sa-AgNPs were studied using TEM imaging. The preparation protocol followed that of the conventional negative staining technique, except that the staining was omitted. In particular, a 5 µL drop of the diluted Sa-AgNPs solution was applied to the surface of a formvar + carbon-coated TEM grid. After attachment of the sample to the film surface (2 minutes), the excess liquid was put away from the edge of grid with filter paper followed by grid drying for five minutes at room temperature. The samples were analyzed as described by Procházková et al. (2018), namely the TEM grids were examined using a JEOL 1011 TEM (JEOL Ltd., Japan) at 80 kV. The microphotographs were taken with a Veleta CCD camera equipped with the Olympus image analysis software (Olympus Soft Imaging Solution, Germany) and were later modified using iTEM 5.1 (Germany Soft Imaging Solution, Germany).

Polydispersity calculation. The pattern of size variation of the Sa-AgNPs was assessed using the polydispersity index, calculated according to Clayton et al. (2016).

Scanning electron microscopy (SEM). The assay was performed to study the surface morphology of the plant-mediated Sa-AgNPs, according to standard protocol for scanning electron microscopy using JEOL JSM-IT800 equipment (JEOL Ltd., Japan). The solution of Sa-AgNPs was repeatedly filtered through a Millipore type Millex filter (0.22 µm). Then, small filter pieces were cut and observed without any coating in HRSEM using 7 kV in SE and BSE imaging. An image of nanoparticles was obtained at a magnification of 100,000 times.

Fourier transform infrared spectroscopy (FTIR). To identify the functional groups of the plant extract that provided the synthesis and stabilization of silver nanoparticles, the cleaned and dried Sa-AgNPs were analyzed. The measurement of the ATR-FTIR spectra was conducted using a Nicolet iS10 spectrometer (Thermo Scientific, USA) linked with a Golden Gate attachment (Specac, UK), at a frequency range of 500–3500 cm^{-1}.

In vitro antibacterial assay. The antibacterial potential of the Sa-AgNPs was assessed using the disc diffusion test (Sharma et al., 2022) against two *S. epidermidis* strains provided by the medical diagnostic institution Centro-Lab (Ukraine) after being clinically isolated from the respiratory tract of different patients, followed by marking with unique internal codes CL1 and CL2, and including in the culture collection of the Microbiology, Virology, and Biotechnology Department of Oles Honchar Dnipro National University. The daily bacterial cultures with CFU 10^9 mL^{-1} were inoculated on a MPA medium in Petri dishes. The solutions of Sa-AgNPs were prepared by two-fold serial dilution in distilled water to obtain the concentrations in a range of 15.625–1000 µg/mL. Sterile paper discs were immersed in the appropriative solutions of Sa-AgNPs and placed on the agar surface. The dishes were incubated at 37 ºC for 24 hours, after which the zone of inhibition (ZOI) around the paper discs (mm, including disc diameter) was measured.

Additionally, the analogous test was conducted to evaluate the susceptibility of both *S. epidermidis* clinical isolates to several commercially available antibiotics of different classes, including fluoroquinolones (inhibitors of DNA synthesis in bacterial cells), cephalosporins (β-lactam antibiotics, inhibitors of the bacterial cell wall synthesis), and aminoglycosides (inhibitors of the bacterial protein synthesis). The study results showed the notable variances in the drug-resistance of the tested clinical bacterial strains of *S. epidermidis* (Table 1).

Table 1
Spectra of the antibacterial drug-resistance of the *S. epidermidis* clinical strains

Antibiotics	Dose, µg/disc	Classes of the drugs	ZOI (mm) of bacterial growth (x ± SD, n = 3)	
			strain CL1	strain CL2
Ofloxacin	5.0	fluoroquinolones	22.04 ± 0.65^{a}	no activity
Levofloxacin	5.0		19.18 ± 0.86^{b}	no activity
Ceftriaxone	30.0	cephalosporins	14.37 ± 0.26^{c}	no activity
Cefuroxime	30.0		9.39 ± 0.18^{d}	no activity
Cefepime	30.0		8.99 ± 0.43^{d}	no activity
Cefoxitin	30.0		9.12 ± 0.44^{d}	no activity
Gentamicin	10.0	aminoglycosides	28.57 ± 1.15^{e}	7.80 ± 0.38^{a}
Amikacin	30.0		22.22 ± 0.81^{fa}	10.09 ± 0.19^{b}

Note: different letters in a column indicate a significant difference in mean values according to the Tukey's test ($P < 0.05$).

The clinical *S. epidermidis* strain CL1 was moderately sensitive to all the tested antibiotics, least of all to cephalosporins, while the strain CL2 was resistant to all the drugs except the aminoglycosides.

Hemolysis assay. An *in vitro* hemolytic test was carried out in accordance with Gul et al. (2021) to assess the toxicity level of the phytosynthesized Sa-AgNPs to human health, specifically, red blood cells (RBCs). In particular, 5 mL of blood with anticoagulant provided by Centro-Lab from a healthy volunteer was centrifuged at 1,500 rpm for 5 min, and plasma was removed, and the residue was washed three times with normal saline and centrifuged in the mode described above. The obtained RBCs were suspended (1:49, v/v) with phosphate buffer solution (PBS), pH 7.4, mixed with Sa-AgNPs solutions (concentration range 200–3.125 µg/mL), and incubated at 37 ºC for 2 hours. Then, the samples were centrifuged at 8,000 rpm for 10 min; and the absorption was measured at 490 nm. The negative (with PBS, pH 7.4) and positive controls (with triton X-100) were prepared according to the procedure described above. The percentage of hemolysis was calculated as: % hemolysis = [(Ds − Dn) / (Dp − Dn)] ×100, where Ds – sample absorption, Dn – negative control absorption, and Dp − positive control absorption.

Statistical analysis. All the assays were repeated at least three times. The microscopic images were taken at least 10 times from different fields of view to obtain the average data. All the data were analyzed using one-way ANOVA, and the results were represented as mean ± standard deviation (x ± SD). The mean values were compared using the Tukey's HSD; and the differences were considered significant at $P \leq 0.05$.

Results

The preparation of silver nanoparticles based on the aqueous extract of *S. aria* leaves (Sa-AgNPs) was visually observed by the color change from light brown of the leaf extract to dark brown of the colloidal solution due to a reduction of Ag^{+} to Ag^{0} in $AgNO_3$ mixed with plant extract (Fig. 1a), and was confirmed by the UV-Visible analysis that revealed the formation of the surface plasmon resonance (SPR) characteristic of metal nanoparticles, with a maximum absorption peak at 450 nm (Fig. 1b).

Electron microscopy techniques, namely TEM and SEM, were applied to study the morphological features and topography of the phytosynthesized Sa-AgNPs at nanometer scale. The transmission electron microscopy of the Sa-AgNPs revealed their sufficiently uniform distribution in the colloidal solution (Fig. 2a), as well as their predominantly spherical and rarely oval shape (Fig. 2b). A micrograph produced by the scanning electron microscopy (Fig. 2c) also showed the spherical shape of the Sa-AgNPs and confirmed the absence of the their aggregation.

The analysis of variability of the Sa-AgNPs sizes, measured using TEM and SEM images, detected that the highest percentage of nanoparticle had a diameter in a range between 30 and 60 nm and an average size of 47.46 ± 17.60 nm (Fig. 2d). The dispersion of the biosynthesized nanoparticles was estimated as moderately polydisperse, based on the polydispersity index calculated as 0.138.

To determine the organic functional groups of phytoconstituents of the *S. aria* leaf extract attached to the surface of biosynthesized silver nanoparticles, we used the FTIR spectroscopy assay (Fig. 3). The spectrum of plant extract had strong bands at 3295.0, 2927.4, 1597.4, 1396.6, 1247.1, and 1064.5 cm^{-1}, as well as some smaller peaks in a range of 887.3–552.6 cm^{-1}. The FTIR spectrum of the Sa-AgNPs showed notable peaks at 3332.9, 2925.4, 2854.9, 2367.7, 1640.9, 1452.6, 1381.1, 1221.9, 1077.4, and 788.8 cm^{-1}.

The antibacterial activity assays, carried out using the disc diffusion test, revealed a moderate sensitivity of the *S. epidermidis* clinically isolated strains to the phytosynthesized silver nanoparticles (Fig. 4).

The biosynthesized Sa-AgNPs produced a dose-dependent growth inhibition of both CL1 and CL2 strains of *S. epidermidis*, which were previously found to be different in the resistance to some antibiotics (Table 2). The hemolytic test conducted with serial dilutions of Sa-AgNPs from 200 to 3.125 µg/mL revealed that the percentage of human RBC hemolysis increased in a dose-dependent manner with rising concentrations of Sa-AgNPs (Table 3).

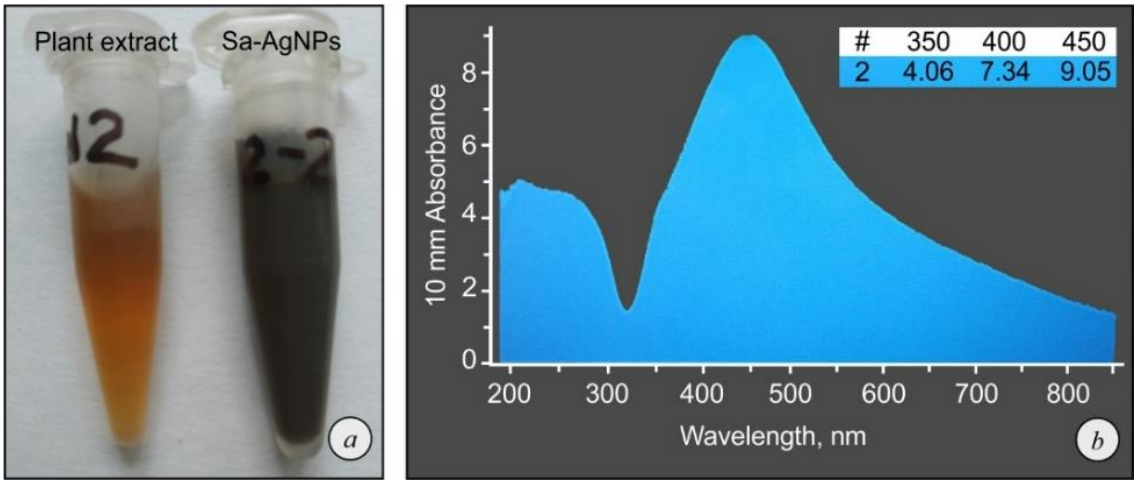

Fig. 1. Primary characterization of the Sa-AgNPs: *a* – visual observation of color change, *b* – UV–Vis spectrum of the Sa-AgNPs

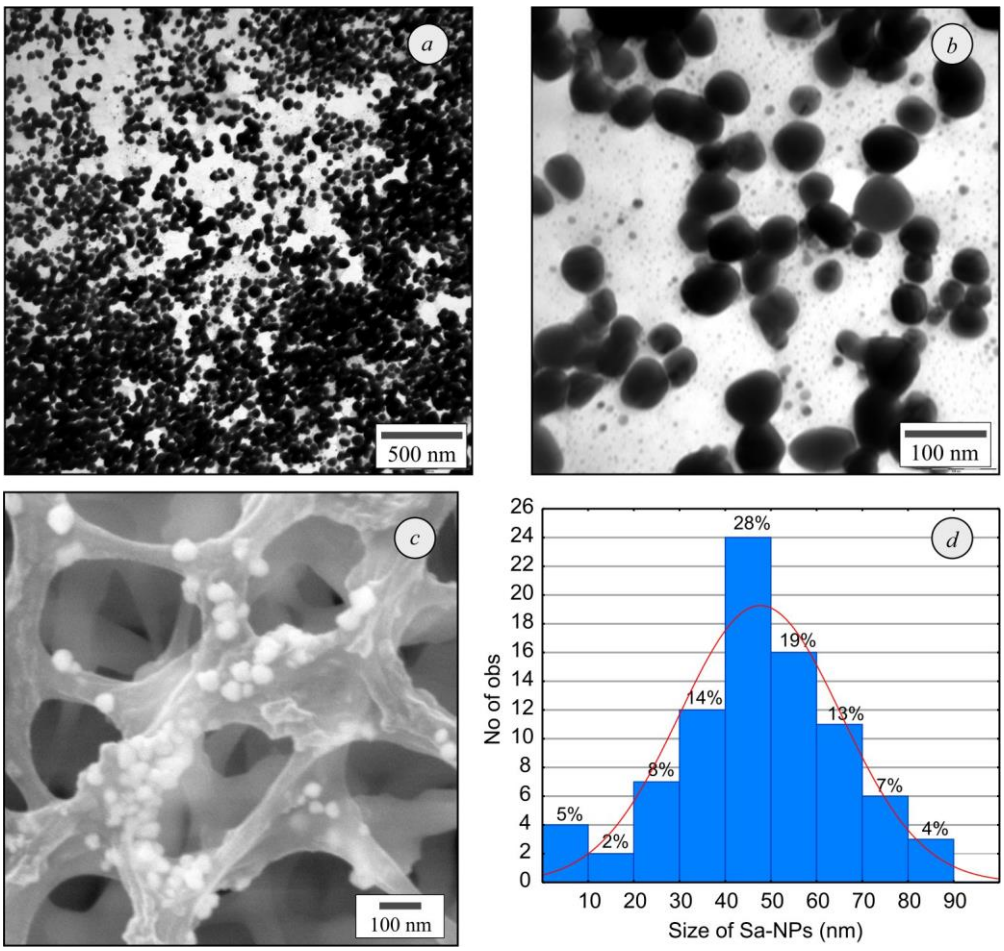

Fig. 2. Electron microscopy assays of the Sa-AgNPs: *a*, *b* – TEM; *c* – SEM imaging; *d* – size distribution histogram

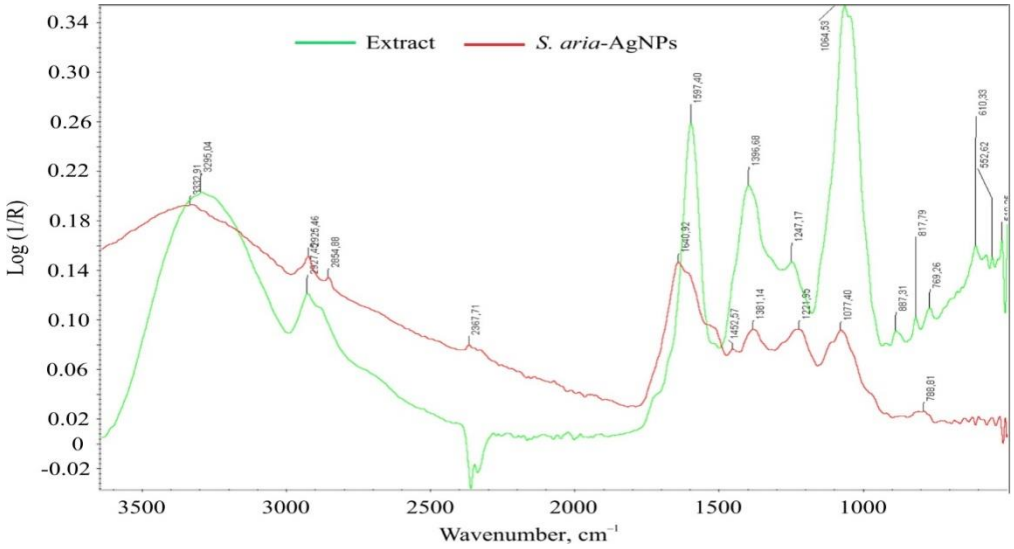

Fig. 3. FTIR spectra of aqueous extract of *S. aria* leaves and the biosynthesized Sa-AgNPs

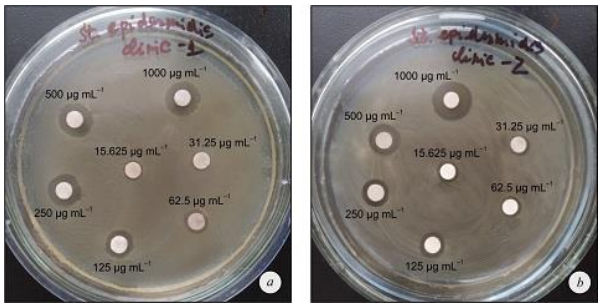

Fig. 4. Antibacterial efficacies of the biosynthesized Sa-AgNPs against *S. epidermidis*: *a* – strain CL1, *b* – strain CL2

Table 2
Inhibition zone diameter of the clinical *S. epidermidis* strains due to Sa-AgNPs action, mm (x ± SD, n =3)

Test-culture	Concentration of *Sa*-AgNPs solution, µg/mL						
	1000.0	500.0	250.0	125.0	62.5	31.25	15.625
Strain CL1	13.59 ± 0.36^{a}	13.20 ± 0.26^{a}	12.83 ± 0.06^{b}	10.89 ± 0.17^{c}	9.35 ± 0.21^{d}	7.82 ± 0.13^{e}	7.46 ± 0.07^{f}
Strain CL2	16.24 ± 0.43^{a}	13.96 ± 0.45^{b}	10.28 ± 0.35^{c}	10.22 ± 0.31^{c}	8.57 ± 0.17^{d}	8.41 ± 0.12^{d}	8.25 ± 0.12^{e}

Note. Different letters in a row indicate a significant difference in means by Tukey's test ($P < 0.05$).

Table 3
Hemolytic activity of the biosynthesized Sa-AgNPs against human RBCs (%, x ± SD, n = 5)

Concentration of *Sa*-AgNPs, µg/mL	200.0	100.0	50.0	25.0	12.5	6.25	3.125
Percentage of hemolysis, %	33.96 ± 1.35^{a}	18.94 ± 0.80^{b}	9.84 ± 0.45^{c}	4.58 ± 0.21^{d}	3.27 ± 0.17^{e}	1.31 ± 0.09^{f}	0.65 ± 0.03^{g}

Note. See Table 2.

Discussion

Biological synthesis of silver nanoparticles, popular among researchers, is often based on leaf extracts of plants, including *Moringa oleifera* (U Din et al., 2024), *Perilla frutescens* (Tavan et al., 2023), *Mentha longifolia* (Adil et al., 2023), and *Enicostemma axillare* (Raj et al., 2018). The plant leaf raw materials are renewable, easily available during the growing season and usually accumulate high content of metabolites, which carry out the direct reduction of silver ions with subsequent formation of silver nanoparticles. In our study, the aqueous leaf extract of *S. aria* plants provided effective reduction, stabilization, and capping of Sa-AgNPs, which were validated by the characteristic peak of surface plasmon resonance (SPR) at 450 nm. The locations of SPR in a close wavelength interval were determined for other plant-derived silver nanoparticles, in particular 415 nm for AgNPs from a *Dovyalis caffra* fruit extract (Al-Rajhi et al., 2022), 430 nm for AgNPs from a *Fritillaria* flower extract (Hemmati, 2019), 442–448 nm for silver nanoparticles from an *Asparagus racemosus* root extract (Amina et al., 2020), and 400–500 nm for different AgNPs derived from *S. aucuparia* fruit extracts (Singh & Mijakovic, 2022).

The electron microscopy used in our study is a common method for determining the surface and morphological characteristics of nanoparticles. The analyses using SEM and TEM validated the production of silver nanoparticles based on *S. aria* leaf extract and provided the topographic and morphological characteristics of the biosynthesized nanoparticles on a nanometer scale. The TEM images of the phytosynthesized Sa-AgNPs showed mostly spherical, non-agglomerated nanoparticles, uniformly distributed in the colloidal solution. The SEM images also demonstrated the predomination of spherical AgNPs and revealed the surface morphology that made it possible to suggest the biological coating surrounding the nanoparticles. A similar assumption was reported about a thick biological corona layer surrounding AgNPs produced by a *S. aucuparia* fruit extract (Singh & Mijakovic, 2022), as well as about the biomolecule coating of the nanoparticles derived from a *D. caffra* fruit extract, molecules of which may attach to the edge of AgNPs and function as chelating agents (Al-Rajhi et al., 2022).

The size of the Sa-AgNPs varied in the range of 30–60 nm and the average size ranged 47.46 ± 17.60 nm. These results are consistent with the published data, including a particle diameter between 40 and 70 nm of the AgNPs biosynthesized using *Salvia verticillata* and *Filipendula ulmaria* extracts (Mihailović et al., 2023), an average size of 12 to 53 nm established for the nanoparticles biosynthesized from *D. caffra* fruit extract (Al-Rajhi et al., 2022), and size variation of 20–30 nm for AgNPs produced using *S. aucuparia* fruit extract (Singh & Mijakovic, 2022). As noted, the polydispersity index was calculated as 0.138, characterizing the moderate polydispersity of the biosynthesized Sa-AgNPs. This value is close to the minimal PDI reported by Reda et al. (2019), specifically, in an interval from 0.149 to 0.982 for silver nanoparticles produced using ginger, garlic, and capsicum extracts. Since the PDI may characterize the nanoparticles stability (Sharma et al., 2022), the moderate polydisperse nature of the biosynthesized Sa-AgNPs may be the reason for absence of their agglomeration.

Phytosynthesis of silver nanoparticles is accompanied by the binding of chemical components of the plant matrix on the surface of AgNPs as blocking and stabilizing agents (Tavan et al., 2023). Identification of the organic functional groups that are attached to the surface of nanoparticles was carried out using Fourier transform infrared spectroscopy. The FTIR spectrum of the Sa-AgNPs showed notable peaks at 3332.9, 2925.4, 2854.9, 2367.7, 1640.9, 1452.6, 1381.1, 1221.9, 1077.4, and 788.8 cm^{-1}. The strong band at 3332.9 cm^{-1} was associated with stretching vibrations of the free –OH groups, indicating the presence of phenols and alcohols (Reddy et al., 2021; Adil et al., 2023). The peaks at 2925.4 and 2854.9 cm^{-1} indicate –CH group stretching of alkanes (Amina et al., 2020; Adil et al., 2023), while the peak at 788.8 cm^{-1} suggests stretching of aromatic compounds (Hossain et al., 2019). The small bands at 2367.7 and 1452.6 cm^{-1} were attributed to the symmetric vibrations of the –COO functional group (Al-Rajhi et al., 2022). The bands at 1640.9 and 1381.1 cm^{-1} were relevant to the stretching vibrations of the –NH group due to the amide linkage (Gul et al., 2021; Al-Rajhi et al., 2022). The indistinct peak at 1602.2 cm^{-1} was attributed to the –C=C– stretching in flavonoids and terpenoids (Singh & Mijakovic, 2022). The peaks at 1221.9 and 1077.4 cm^{-1} represent the stretching vibration of the –C–O group, respectively, in esters and alcohols (Adil et al., 2023).

The comparative analysis revealed the notable differences between the FTIR spectra of Sa-AgNPs and aqueous extract of *S. aria* leaves, namely the wavenumber shift of all bands, and the reduction, appearance, and disappearance of some bands. Sharp decline was observed for the peaks at 3295.0 cm^{-1} (–OH groups of the phenols and alcohols), 1597.4 cm^{-1} (C=C groups of phenols and terpenoids), 1396.6 cm^{-1} (–NH group of proteins), as well as at 1247.1 and 1064.5 cm^{-1} (C–O group of esters and alcohols). The disappearance of some small peaks was revealed in the range 887–552 cm^{-1}, including 887.3 cm^{-1} responsible for the presence of saponins (Amina et al., 2020), 817.7 and 610.3 cm^{-1} represented the bending vibrations of the C–H groups of aromatic rings (Tavan et al., 2023), and 552.6 cm^{-1} indicated the aryl disulfide (S–S) stretching (Sharma et al., 2022). The alterations in the band features in the FTIR spectrum of Sa-AgNPs, as compared with the plant extract spectrum, likely result from the involvement of the correspondeing functional groups of plant metabolites in the biosynthesis of silver nanoparticles. According to the study results, the greatest contribution to the reduction of silver ions and stabilization of nanoparticles have been made by the hydroxyl, carbonyl and carboxyl groups of the phenolics, alcohols, aldehydes, and esters, as well as by the unsaturated double bonds of flavonoids and terpenoids, while amides were important for AgNPs capping. Our findings correlate with the data about stabilization of nanoparticles through the chelation of silver ions by hydroxyl and carbonyl groups of phenolics (Tavan et al., 2023), and about an important role of the NH, CO, and OH groups in the reduction and stability of AgNPs (Al-Rajhi et al., 2022).

Antimicrobial activity appears to be one of the most extensively studied aspects of the unique features of biosynthesized silver nanoparticles. Great hopes of researchers are related to the potential ability of AgNPs to overcome the drug resistance of pathogenic microorganisms that cannot be controlled by existing conventional antibiotics (Vazquez-Muñoz et al., 2019; Adil et al., 2023; Ghai, 2024). The resistant bacterial strains often arise among opportunistic bacteria and can develop polyresistance, as is currently the case with *S. epidermid-*

is (Oliver et al., 2022). Antibiotic-resistant strains of *S. epidermidis* emerge in the healthcare sector. For example, Mazur et al. (2020) isolated nine multidrug-resistant (MDR) clinical strains of *S. epidermidis* from blood cultures. Thomas et al. (2020) reported on a multidrug-resistant and biofilm-forming coagulase-negative *S. epidermidis* strain with a high minimal inhibition concentration of methicillin at a level of 250 µg/mL. Moreover, the undesirable properties of *S. epidermidis* include the ability to serve as a carrier of antibiotic resistance genes among *Staphylococcus* spp. (Xu et al., 2018).

In our study, two different clinically isolated *S. epidermidis* strains CL1 and CL2 showed susceptibility or resistance, respectively, to some common cephalosporins (ceftriaxone, cefuroxime, cefepime, and cefoxitin). The strain CL2 was also resistant to fluoroquinolones (ofloxacin and levofloxacin). Finally, only aminoglycosides achieved the growth inhibition of both *S. epidermidis* clinical strains, with gentamicin being the most effective against the strain CL1 (inhibition zone 28.57 ± 1.15 mm) and amikacin being the most effective against the strain CL2 (inhibition zone 10.09 ± 0.19 mm); the effect of aminoglycosides on the CL2 strain was on average three times weaker than on the CL1 strain. Our findings regarding the multidrug resistance of the CL2 strain are consistent with the data (Ehlers et al., 2018) that all fifty-nine *S. epidermidis* clinical isolates from the hospital in Pretoria were identified as resistant to β-lactams, and had low susceptibility to erythromycin and gentamicin. The high gentamicin activity against the cephalosporin-resistant strains CL1 and CL2 could be an encouraging result if it were not for the side effects of this drug, such as nephrotoxicity, neurotoxicity, ototoxicity, hematological disorders, and impairment of liver function (Mazur et al., 2020), which indicates the need to find alternative means. The antibacterial activity of biosynthesized Sa-AgNPs was exerted against both *S. epidermidis* strains in all tested concentrations, most notably at the doses of 125–1000 µg/mL, producing maximal ZOIs of 13.6 mm for the strain CL1, and 16.2 mm for the strain CL2. As such, the *S. epidermidis* clinical strain CL2, which displayed stronger resistance to several fluoroquinolones, cephalosporines, and aminoglycosides, demonstrated slightly higher susceptibility to the antibacterial action of Sa-AgNPs than the less drug-resistant strain.

The inhibition effects of silver nanoparticles on *S. epidermidis* strains have been revealed in some studies. For example, the museum strain *S. epidermidis* MTCC-2639 was observed to be highly susceptible to AgNPs synthesized using a *Calliandra haematocephala* aqueous leaf extract, with the inhibition zone diameter of 30 mm, compared with only 18 mm zone produced by gentamycin (Nilavukkarasi et al., 2020). The multidrug-resistant *S. epidermidis* strain ATCC 35984 showed susceptibility to the action of AgNPs biosynthesized from a *Fusarium oxysporum* cultural medium, with minimal inhibitory concentration ranging 3.75 to 15 µg/mL and in a dose-dependent manner (da Cunha et al., 2023). At the same time, Mazur et al. (2020) found no antimicrobial activity of tween-stabilized silver nanoparticles (in a range of 21.5 to 1400 µg/mL) against the clinical *S. epidermidis* strains, which indicates the advantages of biosynthesized silver nanoparticles over chemically synthesized ones. The antibacterial effects of AgNPs are realized through the following multilevel mechanisms: penetration via endocytosis; imbalance of membrane potential; binding with bacterial cell surface; generation of reactive oxygen species (ROS); crosslinking with genetic material; nucleic acid disorganization; protein disfunction; and enzyme inactivation (Summer et al., 2024). Therefore, AgNPs are potentially capable of overcoming bacterial resistance to cephalosporins, which arises due to the known (Munita & Arias, 2016) ability of *Staphylococcus* spp. to enzymatically inactivate β-lactam antibiotics by staphylococcal penicillinase, as well as drugs with other modes of action.

In the hemolytic assay, the biosynthesized Sa-AgNPs at the tested concentrations showed the dose-dependent hemolysis of human RBCs in the range 0.65–33.96%. The estimation of the biocompatibility of the nanoparticles at a permissible level of 5% according to the studies (Hossain et al., 2019; Gul et al., 2021) showed an acceptable effect of Sa-AgNPs in a concentration of up to 25.0 µg/mL. Our findings correspond to the study, in which silver nanoparticles biosynthesized from a *Ricinus communis* leaf extract, tested in a concentration range of 2–20 µg/mL, exhibited good biocompatibility (hemolysis at the level of 5.01%) at concentrations of up to 12 µg/mL, while beyond this limit, the percentage of hemolysis exceeded the permissible level (Gul et al., 2021). The dose-dependent hemolysis of human RBCs of less than 5% (the highest 2.60%) was demonstrated by AgNPs biosynthesized based on a *M. longifolia* extract at concentrations ranging 1.25 to 20 µg/mL (Adil et al., 2023). At a concentration of 10–1600 µg/mL, AgNPs derived from *Andrographis paniculata* aqueous steam extract achieved the acceptable percentage of human RBC hemolysis (i.e., 4.56%) of up to 60 µg/mL (Hossain et al., 2019). Silver nanoparticles synthesized with different natural polymers as capping agents showed dose-dependent hemolytic activity in the human whole blood samples and in washed erythrocytes (Srivastava et al., 2021). The data presented above confirm that hemolytic research is an important component of biocompatibility testing of nanomaterials, considering the function of blood as the main carrier of foreign substances, including nanoparticles (Ferdous et al., 2018; Gul et al., 2021). The hemolytic activity of AgNPs is explained by the direct interactions with erythrocytes, where nanoparticles bind to thiol groups of proteins and phospholipids in the erythrocyte membrane, which leads to denaturation and disruption of the membrane functions (de la Harpe et al., 2019). In summary, the hemolytic activity of biosynthesized Sa-AgNPs in the concentration range of 3.125–25.0 µg/mL can be suggested as well biocompatible and acceptable.

Conclusion

The successful phytosynthesis of silver nanoparticles was carried out using the aqueous leaf extract from *S. aria* plants. The biosynthesized Sa-AgNPs were characterized by the means of appropriate techniques, including UV-Vis spectroscopy, electron microscopy (TEM and SEM imaging), and Fourier transform infrared spectroscopy. The surface plasmon resonance at 450 nm, spherical shape, average size 47.46 ± 17.60 nm, and absence of agglomeration were determined for the Sa-AgNPs. Phenolics, alcohols, terpenes, and proteins were identified as the main reducing, stabilizing, and capping agents, and hydroxyl, carbonyl, carboxyl, and amines were the responsible functional groups. The disc diffusion test showed the dose-dependent antibacterial activity of Sa-AgNPs in the concentration range of 15.625–1000 µg/mL against two clinically isolated *S. epidermidis* strains differeing in the resistance to several cephalosporins, fluoroquinolones, and aminoglycosides. The hemolytic test showed good biological compatibility of Sa-AgNPs at concentrations of up to 25 µg/mL. The obtained results confirmed the potential ability of phytosynthesized Sa-AgNPs to achieve considerable success in the fight against antibiotic resistance of *S. epidermidis*. However, the suitability of Sa-AgNPs for the development of new antibacterial drugs requires further research testing a larger number of resistant clinical strains. In addition, research may also aim to identify the phytochemicals of *S. aria* leaf extract involved in the biosynthetic process to produce Sa-AgNPs.

The authors declare no conflict of interest.

We thank the Viničná Microscopy Core Facility (VMCF of the Faculty of Science, Charles University), an institution supported by the MEYS CR (LM2023050 Czech-BioImaging) for their support & assistance in this work.

The study was carried out within the scope of the research work "Application of nanoparticles based on plant matrices to enhance the antimicrobial effects of phytocompounds against resistant pathogens" as part of the scientific and technical work "Implementation of the tasks of the perspective plan for the development of the scientific direction "Biology and health care" (state registration number 0122U000059, 2021–2025).

Lenka Procházková was supported by University Research Centers (UNCE) at the Charles University No. UNCE/24/SCI/006.

References

Adil, M., Alam, S., Amin, U., Ullah, I., Muhammad, M., Ullah, M., Rehman, A., & Khan T. (2023). Efficient green silver nanoparticles-antibiotic combinations against antibiotic-resistant bacteria. AMB Express, 13, 115.

Aguirre, D. P. R., Loyola, E. F., De la Fuente Salcido, N. M., Sifuentes, L. R., Moreno, A. R., & Jolas, J. E. M. (2020). Comparative antibacterial potential of silver nanoparticles prepared via chemical and biological synthesis. Arabian Journal of Chemistry, 13, 8662–8670.

Akhter, S., Rahman, A., Ripon, R.K., Mubarak, M., Akter, M., Mahbub, S., Al Mamun, F., & Sikder, T. (2024). A systematic review on green synthesis of silver nanoparticles using plants extract and their bio-medical applications. Heliyon, 10(11), e29766.

Al-Rajhi, A. M. H., Salem, S. S., Alharbi, A. A., & Abdelghany, T. M. (2022). Ecofriendly synthesis of silver nanoparticles using Kei-apple (*Dovyalis caffra*) fruit and their efficacy against cancer cells and clinical pathogenic microorganisms. Arabian Journal of Chemistry, 15(7), 103927.

Amina, M., Al Musayeib, N. M., Alarfaj, N. A., El-Tohamy, M. F., & Al-Hamoud, G. A. (2020). Antibacterial and immunomodulatory potentials of biosynthesized Ag, Au, Ag-Au bimetallic alloy nanoparticles using the *Asparagus racemosus* root extract. Nanomaterials, 10, 2453.

Arvinte, O. M., Senila, L., Becze, A., & Amariei, S. (2023). Rowanberry – a source of bioactive compounds and their biopharmaceutical properties. Plants, 12(18), 3225.

Asante, J., Hetsa, B. A., Amoako, D. G., Abia, A. L. K., Bester, L. A., & Essack, S. Y. (2021). Genomic analysis of antibiotic-resistant *Staphylococcus epidermidis* isolates from clinical sources in the Kwazulu-Natal Province, South Africa. Frontiers in Microbiology, 12, 656306.

Bobinaitė, R., Grootaert, C., Van Camp, J., Šarkinas, A., Liaudanskas, M., Žvikas, V., Viškelis, P., & Venskutonis, P. R. (2020). Chemical composition, antioxidant, antimicrobial and antiproliferative activities of the extracts isolated from the pomace of rowanberry (*Sorbus aucuparia* L.). Food Research International, 136, 109310.

Clayton, K. N., Salameh, J. W., Wereley, S. T., & Kinzer-Ursem, T. L. (2016). Physical characterization of nanoparticle size and surface modification using particle scattering diffusometry. Biomicrofluidics, 10(5), 054107.

Cook, M. A., & Wright, G. D. (2022). The past, present, and future of antibiotics. Science Translational Medicine, 14(657), eabo7793.

da Cunha, K. F., Oliveira Garcia, M., Allend, S. O., de Albernaz, D. F. T., Panagio, L. A., Seixas Neto, A. C. P., Oliveira, T. L., & Hartwig, D. D. (2023). Biogenic silver nanoparticles: *In vitro* activity against *Staphylococcus aureus* methicillin-resistant (MRSA) and multidrug-resistant coagulase-negative *Staphylococcus* (CoNS). Brazilian Journal of Microbiology, 54, 2641–2650.

de la Harpe, K. M., Kondiah, P. D. P., Choonara, Y. E., Marimuthu, T., du Toit, L. C., & Pillay, V. (2019). The hemocompatibility of nanoparticles: A review of cell–nanoparticle interactions and hemostasis. Cells, 8(10), 1209.

Didur, O. O., Khromykh, N. O., Drehval, O. A., Sklyar, T. V., Dzhagan, V. M., Mazur, N. V., Skoryk, M. A., & Kurahina, N. V. (2024). Influence of silver nanoparticles synthesized from *Chaenomeles* leaf extracts on pathogens microorganisms *Klebsiella pneumoniae*, *Staphylococcus aureus*, and *Fusarium culmorum*. Biosystems Diversity, 3(3), 380–388.

Ehlers, M. M., Strasheim, W., Lowe, M., Ueckermann, V., & Kock, M. M. (2018). Molecular epidemiology of *Staphylococcus epidermidis* implicated in catheter-related bloodstream infections at an Academic Hospital in Pretoria, South Africa. Frontiers in Microbiology, 9, 417.

Ewunkem, A. J., Williams, Z. J., Johnson, N. S., Brittany, J. L., Maselugbo, A., & Nowlin, K. (2023). Exploring the "Carpenter" as a substrate for green synthesis: Biosynthesis and antimicrobial potential. Gene and Protein in Disease, 2(4), 2155.

Ferdous, Z., Beegam, S., Tariq, S., Ali, B. H., & Nemmar, A. (2018). The *in vitro* effect of polyvinylpyrrolidone and citrate coated silver nanoparticles on erythrocytic oxidative damage and eryptosis. Cellular Physiology and Biochemistry, 49(4), 1577–1588.

Ghai, I. (2024). Electrophysiological insights into antibiotic translocation and resistance: The impact of outer membrane proteins. Membranes, 14(7), 161.

Gul, A., Fozia, Shaheen, A., Ahmad, I., Khattak, B., Ahmad, M., Ullah, R., Bari, A., Ali, S. S., Alobaid, A., Asmari, M. M., & Mahmood, H. M. (2021). Green synthesis, characterization, enzyme inhibition, antimicrobial potential, and cytotoxic activity of plant mediated silver nanoparticle using *Ricinus communis* leaf and root extracts. Biomolecules, 11(2), 206.

Hemmati, S., Rashtiani, A., Zangeneh, M. M., Mohammadi, P., Zangeneh, A., & Veisi, H. (2019). Green synthesis and characterization of silver nanoparticles using *Fritillaria* flower extract and their antibacterial activity against some human pathogens. Polyhedron, 158, 8–14.

Hossain, M. M., Polash, S. A., Takikawa, M., Shubhra, R. D., Saha, T., Islam, Z., Hossain, S., Hasan, M. A., Takeoka, S., & Sarker, S. R. (2019). Investigation of the antibacterial activity and *in vivo* cytotoxicity of biogenic silver nanoparticles as potent therapeutics. Frontiers in Bioengineering and Biotechnology, 7, 239.

Karan, T., Gonulalan, Z., Erenler, R., Kolemen, U., & Eminagaoglu, O. (2024). Green synthesis of silver nanoparticles using *Sambucus ebulus* leaves extract: Characterization, quantitative analysis of bioactive molecules, antioxidant and antibacterial activities. Journal of Molecular Structure, 1296(1), 136836.

Khan, M. H., Unnikrishnan, S., & Ramalingam, K. (2024). Antipathogenic efficacy of biogenic silver nanoparticles and antibiofilm activities against multi-drug-resistant ESKAPE pathogens. Applied Biochemistry and Biotechnology, 196, 2031–2052.

Lykholat, Y. V., Khromykh, N. O., Anishchenko, A. O., Didur, O. O., Koptieva, S. D., Sklyar, T. V., & Liashenko, O. V. (2024). Chemotaxonomic significance assessment of phytochemical heterogeneity of the genus *Sorbus* inflorescences. Journal of Chemistry and Technologies, 32(2), 267–275.

Lykholat, Y. V., Khromykh, N. O., Didur, O. O., Sklyar, T. V., Balalaiev, O. K., Borova, M. M., Dzhagan, V. M., & Yemets, A. I. (2025). *Chaenomeles japonica* mediated fabrication of silver nanoparticles and their conjugates with ceftriaxone: Characterization and antibacterial effect. Cytology and Genetics, 59(1), 1–10.

Mazur, P., Skiba-Kurek, I., Mrowiec, P., Karczewska, E., & Drożdż, R. (2020). Synergistic ROS-associated antimicrobial activity of silver nanoparticles and gentamicin against *Staphylococcus epidermidis*. International Journal of Nanomedicine, 15, 3551–3562.

Mihailović, V., Srećković, N., Nedić, Z. P., Dimitrijević, S., Matić, M., Obradović, A., Selaković, D., Rosić, G., & Stanković, J. S. K. (2023). Green synthesis of silver nanoparticles using *Salvia verticillata* and *Filipendula ulmaria* extracts: Optimization of synthesis, biological activities, and catalytic properties. Molecules, 28(2), 808.

More, P. R., Pandit, S., Filippis, A. D., Franci, G., Mijakovic, I., & Galdiero, M. (2023). Silver nanoparticles: Bactericidal and mechanistic approach against drug resistant pathogens. Microorganisms, 11(2), 369.

Munita, J. M., & Arias, C. A. (2016). Mechanisms of antibiotic resistance. Microbiology Spectrum, 4(2), 2015.

Nilavukkarasi, M., Vijayakumar, S., & Kumar, S. P. (2020). Biological synthesis and characterization of silver nanoparticles with *Capparis zeylanica* L. leaf extract for potent antimicrobial and anti-proliferation efficiency. Materials Science for Energy Technologies, 3, 371–376.

Oliver, L. V., Calduch, P. B., Rodríguez, L. F., Ortega, D. N., Samper, A. M. D., & Rodríguez, J. C. (2022). Methicillin-resistant *Staphylococcus epidermidis* infectious keratitis: Clinical and microbiological profile. Revista Española de Quimioterapia, 35(2), 171–177.

Orsavová, J., Juríková, T., Bednaříková, R., & Mlček, J. (2023). Total phenolic and total flavonoid content, individual phenolic compounds and antioxidant activity in sweet rowanberry cultivars. Antioxidants, 12(4), 913.

Osman, A. I., Zhang, Y., Farghali, M., Rashwan, A. K., Eltaweil, A. S., El-Monaem, E. M. A., Mohamed, I. M. A., Badr, M. M., Ihara, I., Rooney, D. W., & Yap, P.-S. (2024). Synthesis of green nanoparticles for energy, biomedical, environmental, agricultural, and food applications: A review. Environmental Chemistry Letters, 22, 841–887.

Paul, D., Chawla, M., Ahrodia, T., Narendrakumar, L., & Das, B. (2023). Antibiotic potentiation as a promising strategy to combat macrolide resistance in bacterial pathogens. Antibiotics, 12(12), 1715.

Procházková, L., Remias, D., Řezanka, T., & Nedbalová, L. (2018). *Chloromonas nivalis* subsp. *tatrae*, subsp nov. (Chlamydomonadales, Chlorophyta): Re-examination of a snow alga from the High Tatra Mountains (Slovakia). Fottea, 18(1), 1–18.

Raj, S., Mali, S. C., & Trivedi, R. (2018). Green synthesis and characterization of silver nanoparticles using *Enicostemma axillare* (Lam.) leaf extract. Biochemical and Biophysical Research Communications, 503(4), 2814–2819.

Reda, M., Ashames, A., Edis, Z., Bloukh, S., Bhandare, R., & Abu Sara, H. (2019). Green synthesis of potent antimicrobial silver nanoparticles using different plant extracts and their mixtures. Processes, 7(8), 510.

Reddy, N. V., Li, H., Hou, T., Bethu, M. S., Ren, Z., & Zhang, Z. (2021). Phytosynthesis of silver nanoparticles using *Perilla frutescens* leaf extract: Characterization and evaluation of antibacterial, antioxidant, and anticancer activities. International Journal of Nanomedicine, 16, 15–29.

Rutkowska, M., Owczarek, A., Kolodziejczyk-Czepas, J., Michel, P., Piotrowska, D. G., Kapusta, P., Nowak, P., & Olszewska, M. A. (2019). Identification of bioactivity markers of *Sorbus domestica* leaves in chromatographic, spectroscopic and biological capacity tests: Application for the quality control. Phytochemical Letters, 30, 278–287.

Salem, S. S. (2023). A mini review on green nanotechnology and its development in biological effects. Archives of Microbiology, 205, 128.

Sánchez-López, E., Gomes, D., Esteruelas, G., Bonilla, L., Lopez-Machado, A. L., Galindo, R., Cano, A., Espina, M., Ettcheto, M., Camins, A., Silva, A. M., Durazzo, A., Santini, A., Garcia, M. L., & Souto, E. B. (2020). Metal-based nanoparticles as antimicrobial agents: An overview. Nanomaterials, 10(2), 292.

Sarv, V., Venskutonis, P. R., & Bhat, R. (2020). The *Sorbus* spp. – underutilised plants for foods and nutraceuticals: Review on polyphenolic phytochemicals and antioxidant potential. Antioxidants, 9(9), 813.

Sharma, A., Sagar, A., Rana, J., & Rani, R. (2022). Green synthesis of silver nanoparticles and its antibacterial activity using fungus *Talaromyces purpureogenus* isolated from *Taxus baccata* Linn. Micro and Nano Systems Letters, 10, 2.

Singh, P., & Mijakovic, I. (2022). Rowan berries: A potential source for green synthesis of extremely monodisperse gold and silver nanoparticles and their antimicrobial property. Pharmaceutics, 14, 82.

Sołtys, A., Galanty, A., & Podolak, I. (2020). Ethnopharmacologically important but underestimated genus *Sorbus*: A comprehensive review. Phytochemistry Reviews, 19, 491–526.

Srivastava, P., Gunawan, C., Soeriyadi, A., Amal, R., Hoehn, K., & Marquis, C. (2021). *In vitro* coronal protein signatures and biological impact of silver nanoparticles synthesized with different natural polymers as capping agents. Nanoscale Advances, 3(15), 4424–4439.

Summer, M., Ali, S., Tahir, H. M., Abaidullah, R., Fiaz, U., Mumtaz, S., Fiaz, H., Hassan, A., Mughal, T. A., & Farooq, M. A. (2024). Mode of action of biogenic silver, zinc, copper, titanium and cobalt nanoparticles against antibiotics resistant pathogens. Journal of Inorganic and Organometallic Polymers and Materials, 34, 1417–1451.

Tahirovic, A., Mehic, E., Kjosevski, N., & Bašic, N. (2019). Phenolics content and antioxidant activity of three *Sorbus* species. Bulletin of the Chemists and Technologists of Bosnia and Herzegovina, 53, 15–21.

Tas, A., Gundogdu, M., Ercisli, S., Orman, E., Celik, K., Marc, R. A., Buckova, M., Adamkova, A., & Micek, J. (2023). Fruit quality characteristics of service tree (*Sorbus domestica* L.) genotypes. ACS Omega, 8(22), 19862–19873.

Tavan, M., Hanachi, P., Mirjalili, M. H., & Dashtbani-Roozbehani A. (2023). Comparative assessment of the biological activity of the green synthesized silver nanoparticles and aqueous leaf extract of *Perilla frutescens* (L.). Scientific Reports, 13, 6391.

Thomas, R., Jishma, P., Snigdha, S., Soumya, K. R., Mathew, J., & Radhakrishnan, E. K. (2020). Enhanced antimicrobial efficacy of biosynthesized silver nanoparticle based antibiotic conjugates. Inorganic Chemistry Communications, 117, 107978.

U Din, M. M., Batool, A., Ashraf, R. S., Yaqub, A., Rashid, A., & U Din, N. M. (2024). Green synthesis and characterization of biologically synthesized and antibiotic-conjugated silver nanoparticles followed by post-synthesis assessment for antibacterial and antioxidant applications. ACS Omega, 9(17), 18909–18921.

Vazquez-Muñoz, R., Meza-Villezcas, A., Fournier, P., Soria-Castro, E., Juarez-Moreno, K., Gallego-Hernández, A., Bogdanchikova, N., Vazquez-Duhalt, R., Huerta-Saquero, A. (2019). Enhancement of antibiotics antimicrobial activity due to the silver nanoparticles impact on the cell membrane. PLoS One, 14(11), e0224904.

Wiart, C., Kathirvalu, G., Raju, C. S., Nissapatorn, V., Rahmatullah, M., Paul, A. K., Rajagopal, M., Seelan, J. S. S., Rusdi, N. A., Scholastica Lanting, S., & Sulaiman, M. (2023). Antibacterial and antifungal terpenes from the medicinal angiosperms of Asia and the Pacific: Haystacks and gold needles. Molecules, 28(9), 3873.

Xu, Z., Misra, R., Jamrozy, D., Paterson, G. K., Cutler, R. R., Holmes, M. A., Gharbia, S., & Mkrtchyan, H. V. (2018). Whole genome sequence and comparative genomics analysis of multi-drug resistant environmental *Staphylococcus epidermidis* ST59. G3: Genes, Genomes, Genetics, 8(7), 2225–2230.

Yadav, A., & Yadav, K. (2025). Nano-enhanced peptides: Bridging cutting-edge tech and biology to outsmart resilient microbes. Academia Nano: Science, Materials, Technology, 2(1), 1–29.